Growth by the μ-PD Method and Visible Laser Operation of a Single-Crystal Fiber of Pr^{3+}:KY_3F_{10}

Jun Shu [1,2], Eugenio Damiano [1,3,*], Alberto Sottile [1,4] ⓘD, Zhonghan Zhang [1,5] and Mauro Tonelli [1,4]

[1] Dipartimento di Fisica, Università di Pisa, Largo B. Pontecorvo 3, 56127 Pisa, Italy; shujunsdu2012@yahoo.com (J.S.); sottile@df.unipi.it (A.S.); zhangzhsunrise@gmail.com (Z.Z.); mauro.tonelli@unipi.it (M.T.)

[2] State Key Laboratory of Crystal Materials, Shandong University, 27 South Shanda Road, Jinan 250100, China

[3] Dipartimento di Scienze Fisiche, della Terra e dell'Ambiente—Sezione di Fisica, Università di Siena, Via Roma 56, 53100 Siena, Italy

[4] NEST, Istituto Nanoscienze—CNR, Piazza S. Silvestro 12, 56127 Pisa, Italy

[5] PSL Research University, Chimie ParisTech, CNRS, Institut de Recherche de Chimie Paris, 11 Rue Pierre et Marie Curie, 75005 Paris, France

* Correspondence: eu.damiano@gmail.com; Tel.: +39-050-2214287

Abstract: We report on the first growth, spectroscopy, and visible laser operation of a single-crystal fiber (SCF) of KY_3F_{10} (KYF) grown by the micro-pulling-down (μ-PD) method, doped with Pr^{3+} ions. This material has a cubic lattice, which makes it appealing for use in the industry. However, KYF crystals are considered difficult to grow with high optical quality, even with well-established methods. Nevertheless, we grew a 50-mm-long SCF of Pr:KYF, which was transparent in its inner part. We studied the spectroscopic features of it in comparison with existing literature and with samples of the same crystal grown by the Czochralski method, and we did not notice any large differences. These characterizations confirmed that is indeed possible to grow high-quality crystals of Pr:KYF by the μ-PD method. Unfortunately, the crystal proved to be more brittle than typical KYF and especially difficult to polish, leading to rough and irregular facets, as evidenced by transmission measurements. Despite these issues, we obtained continuous-wave laser operation in the orange, red, and deep red regions, using a sample carved from the SCF as active medium and an InGaN-based laser diode as pump source, though with lower performances than in existing reports on this crystal.

Keywords: solid-state lasers; visible lasers; single-crystal fibers; spectroscopy; micro-pulling-down; crystal growth; diode-pumped lasers; laser materials; praseodymium-based lasers

1. Introduction

Visible laser applications are now ubiquitous in our society, ranging from medicine to entertainment, and from industry to fundamental scientific research. Nevertheless, broad regions in the visible part of the electromagnetic spectrum are still uncovered by compact and stable laser sources. Solid-state lasers based on Pr^{3+} ions are extremely interesting in this context, thanks to their various transitions, which can be exploited to achieve visible laser emissions without using complex solutions, such as second harmonic generation [1–4]. Among the possible hosts for Pr^{3+} ions, fluorides had proven to be the best option. Fluoride single crystals benefit from a lower phonon energy with respect to the widely used oxide materials (e.g. yttrium aluminum garnet and yttrium orthovanadate), preventing detrimental non-radiative decays. Moreover, Pr^{3+} ions embedded in fluoride hosts do not exhibit any excited state absorption nor cooperative processes, at least at low doping levels [5].

Potassium triyttrium decafluoride (chemical formula KY_3F_{10}, shortened as KYF) is a promising laser material. The interest in this crystal is mainly justified by its cubic structure, which allows its

orientation to be disregarded in solid-state laser operations. Its isotropy is also expected to simplify the storage and handling of this crystal in industrial applications. The most common technique to grow rare-earth-doped fluorides is the Czochralski (CZ) method, which allows the growth of large single crystals with remarkable optical quality. Unfortunately, due to detrimental processes that affect the growth, KYF is struggling to emerge as an appealing laser material. Only in recent years has a reliable procedure to grow this material by the CZ method been developed and patented [6]. After this innovation was introduced, rare-earth-doped KYF crystals have shown remarkable results in laser operation [7]. In particular, visible laser emission in CZ-grown Pr-doped KYF (Pr:KYF) has been reported using many transitions [8,9].

However, CZ-grown boules of KYF cannot be mechanically reduced to obtain millimeter-sized samples suitable, for example, for compact optoelectronic devices. These issues can be overcome by using the micro-pulling-down (μ-PD) method. This technique enables the growth of cylindrical-shaped crystals with diameters as low as 500 μm [10,11], achieving transverse sizes that are unreachable by mechanical processing in such brittle materials. These cylindrical monocrystalline rods are usually called single-crystal fibers (SCFs). Moreover, the quantity of raw materials required to perform the growth is significantly smaller than in the CZ technique, and the amount of wasted material for each growth is, in principle, negligible.

Recently, Pr-doped μ-PD-grown fluoride SCFs have been proven capable of sustaining visible laser operation [12,13], using uniaxial crystals. However, the growth of uniaxial materials for laser applications imposes strict requirements on the orientation of the crystal lattice. KYF, on the other hand, does not require a specific orientation, thanks to its cubic structure. In this paper, we report on the first growth of a SCF of KYF by means of the μ-PD technique. We performed a complete spectroscopic characterization in terms of absorption and fluorescence spectra, both static and dynamic. We achieved diode-pumped laser operation in a Pr:KYF SCF, for the first time to the best of our knowledge, in the orange, red, and deep red regions.

2. Materials and Methods

2.1. Crystal Structure and Growth

Crystalline KYF has a cubic structure. Its space group is $Fm\bar{3}m$, with unit cell parameter a = 11.5439 Å. Each cell contains eight formula units. When doped with rare earths, the substitution $Y^{3+} \rightarrow RE^{3+}$ takes place, filling a C_{4v} symmetry site [14,15]. Having a cubic lattice, all the optical and structural properties of this crystal are expected to be the same along any direction of incidence.

The growth was performed in a custom-made RF-heated μ-PD furnace located in our laboratories in Pisa. We used PrF_3 and KY_3F_{10} as starting materials, weighted to obtain a 1 at.% doping level. Raw materials had a purity of 99.999% (5N) and were supplied by AC Materials (Tarpon Springs, FL, USA). We employed a glass-like carbon crucible for the growth. The crucible had a cylindrical shape with a conical narrowing in the lower part and a 1.3-mm-wide aperture at the end of it, from which the crystal was extracted. We inserted 3 g of starting powders into the crucible. The growth was carried out at about 1000 °C in an inert argon atmosphere at 0.9 atm. Since the orientation was not expected to affect the absorption efficiency, given the cubic structure of KYF, the use of an oriented single-crystal seed to start the growth and preselect the orientation was unnecessary. Therefore, we employed a high-purity platinum wire as seed. After starting the growth, the pulling rate was set to 1.5 mm/h. We successfully grew a 50-mm-long SCF with a constant diameter of 1.6 mm. Unfortunately, the fiber detached from the crucible during the cooling phase and broke. We recovered two 20-mm-long parts still intact (Figure 1a), from which we obtained all the samples studied in this work.

Upon visual inspection, it can be seen that the external surface of the fiber had a whitish appearance, probably because of the deposition of lighter fluorides, while the inner channel looked transparent (Figure 1b), and therefore was suitable for optical applications. Several cylindrical samples were cut from the fiber, and their circular facets were polished for the subsequent characterizations.

Unfortunately, the grown crystal was particularly brittle, even in comparison with CZ-grown KYF crystals. This brittleness resulted in difficulties in manipulating and polishing the samples, preventing us from getting regular and plane surfaces and giving rise to non-parallelism between the circular facets of the polished samples carved from the SCF. Furthermore, during growth, Pr-doped materials are affected by the phenomenon of segregation, which prevents the doping ions from entering efficiently in the lattice sites of the host, leading to an effective doping level lower than the one intended [16]. For this reason, it was not possible to estimate the actual Pr^{3+} doping level in the crystal.

| (a) | (b) |
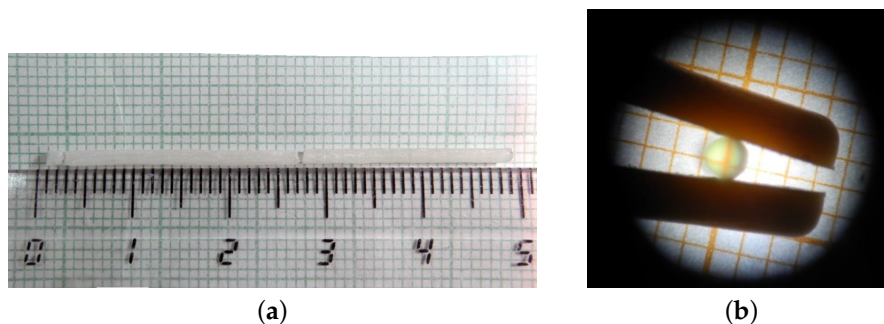
Figure 1. (**a**) Picture of the as-grown Pr-doped KY_3F_{10} (KYF) (Pr:KYF) single crystal fiber (SCF). (**b**) Transverse cross-section of a 25-mm-long section of the same fiber, seen through a microscope.

2.2. Structural Characterization

Even if we were not interested in the orientation of the crystal lattice (since it should have not influenced the optical properties), we employed an X-ray Laue diffractometer to study the crystal structure and verify the single-crystal nature of the samples. We observed that the whole fiber was indeed a single crystal by targeting different parts of the grown crystal.

The optical quality of a 3.9-mm-long sample was studied by observing the propagation through the SCF of a TEM_{00} mode of an He-Ne laser, selected with a spatial filter, as described in [17]. We used the sample that we later employed during laser experiments. The transmitted beam was detected by means of a CCD camera. With this setup, we also estimated the wedge angle between the circular facets of the SCF.

2.3. Spectroscopy

We performed a full spectroscopic characterization of the Pr:KYF SCF at room temperature. In all measurements discussed below, we disregarded the polarization of incident and emitted light, since KYF is expected to be isotropic. The absorption spectrum was measured in the range 350–560 nm with a resolution of 0.15 nm, by means of a Varian Cary 500 spectrophotometer. Steady-state fluorescence spectra were acquired in the range 465–750 nm by pumping the SCF with an InGaN-based laser diode at 445 nm. The fluorescence light—collected perpendicularly to the incident beam—was sent into a monochromator and detected with a photomultiplier. We acquired the emission data between 465 and 750 nm, with a resolution of 0.13 nm. The fluorescence decay time of the $^3P_0$ level was measured by pumping the sample with a pulsed frequency-doubled Ti:Sapphire laser, with a pulse width of 30 ns and a repetition rate of 10 Hz. The decay profile was detected with the same setup employed in steady-state fluorescence measurement.

2.4. Laser

For our laser experiments, we employed a resonant hemispherical cavity. The complete setup for laser experiments is shown in Figure 2. The flat mirror M1 was anti-reflectively coated for the incident pump light (420–520 nm) and was highly reflective in the output laser region (590–750 nm). We used different M2 mirrors to select the emission line and the extraction of photons from the cavity.

The radius of curvature of the M2 mirror was 100 mm for the operations in the orange line and 50 mm for the operations in the red and deep red regions. For each choice of the M2 mirror, we set the length of the cavity approximately equal to the radius of curvature of the mirror, and we refined the alignment to get the maximum output power. A 3.9-mm-long sample was glued, with a suitable thermal-conductive adhesive, on a custom copper holder with a V-shaped valley, designed to accommodate a cylindrical sample. The holder was mounted on a goniometric head, and it was cooled by recirculating water at about 15 °C. We did not apply any coating to the circular facets of the laser sample. The whole holding system was placed as close as possible to the mirror M1. We utilized an InGaN-based laser diode (LD) emitting at 445 nm as pump source. This wavelength is slightly detuned with respect to the center of the absorption peak because at the time of the measurement, an InGaN-based diode capable of emitting at 446 nm was not available in our laboratories. This detuning, together with the impossibility of efficiently preparing longer laser samples, led to a single-pass absorption efficiency η_{abs} of about 50%. The divergence of the pump beam was corrected with a collimator (CL), and the astigmatism was corrected with a pair of cylindrical lenses (CYL). To continuously tune the power incident in the cavity, we used a combination of a $\lambda/2$-plate (HW) and a polarizing beam-splitter cube (PBS). The pump beam was focused on the sample by an achromatic lens (FL) with a focal length of 35 mm. Additionally, in this case, we disregarded the polarization of the light incident on the sample. Using two silicon-based power meters (PM), we measured the input power and the output power simultaneously. Since the M2 mirrors were not completely reflective to the pump light, we placed a long-pass filter behind the output coupler to eliminate the residual pump light.
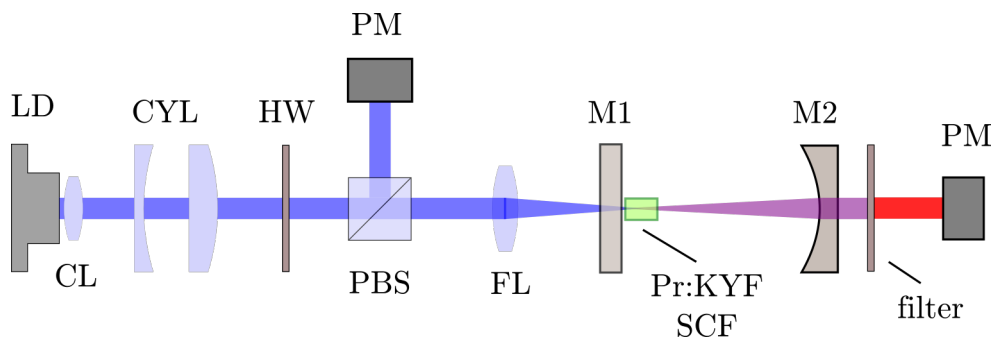
Figure 2. Scheme of the setup employed for laser operation. The components are described in the text. LD: laser diode; CL: collimator; CYL: cylindrical lenses; HW: $\lambda/2$-plate; PBS: polarizing beam-splitter cube; FL: achromatic lens; M1,M2: mirrors; PM: power meter.

3. Results

3.1. Structural Characterization

From the transmission measurements on the laser sample, we observed that the crystal introduced severe distortions in the shape and in the intensity profile of the transmitted beam. Since no significant transmission intensity losses were observed, we believe that these distortions were due to the poor polishing of the circular facets, which produced curved surfaces instead of flat. Moreover, the wedge angle between the circular facets of the laser sample was estimated to be about 2°.

3.2. Spectroscopy

From Figure 3a, which shows the absorption spectrum the blue, green, and yellow regions, we can spot the presence of a parasitic background absorption. By successfully fitting this background with an inverse-fourth-power law, we can infer that it was due to the Rayleigh scattering inside the SCF. Nevertheless, the effect of internal scattering is expected to be negligible in orange, red, and deep red regions in which we are interested. The absorption spectrum discussed before, after subtracting the fitted background, is alike to the spectrum of a CZ-grown sample of Pr:KYF, as can be seen in

Figure 3b. This similarity is an indication that the doping ions correctly entered in the right sites of the crystal lattice. In our SCF, the absorption peak accessible to InGaN-based laser diodes lies at 446 nm, the same as in the CZ-grown KYF.
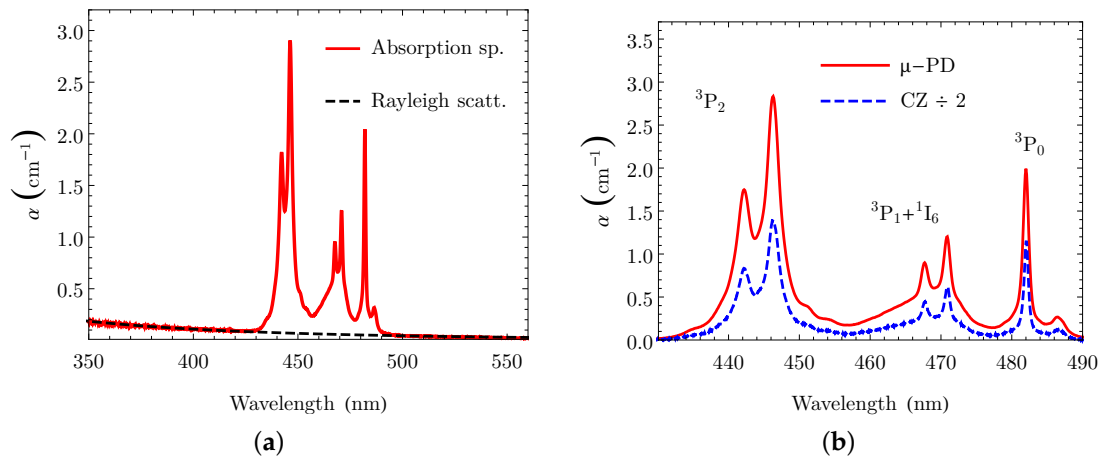
Figure 3. (**a**) Absorption spectrum of the Pr:KYF SCF in the blue, green, and yellow regions. The dashed curve shows the fit of the background Rayleigh scattering. (**b**) Corrected absorption spectrum of the SCF in comparison with a crystal grown by the Czochralski (CZ) method (scaled for clarity). μ-PD: micro-pulling-down.

The fluorescence spectrum of the Pr:KYF SCF was recorded and corrected for the optical response of the setup, determined using an Ocean Optics HL-3plus-INT-CAL calibration lamp. Figure 4 shows the acquired fluorescence spectrum in the orange, red, and deep red regions, in comparison with the same spectrum from a CZ-grown sample of Pr:KYF, scaled to avoid superposition. We can observe that the spectra of the two samples grown by the two different techniques are identical.
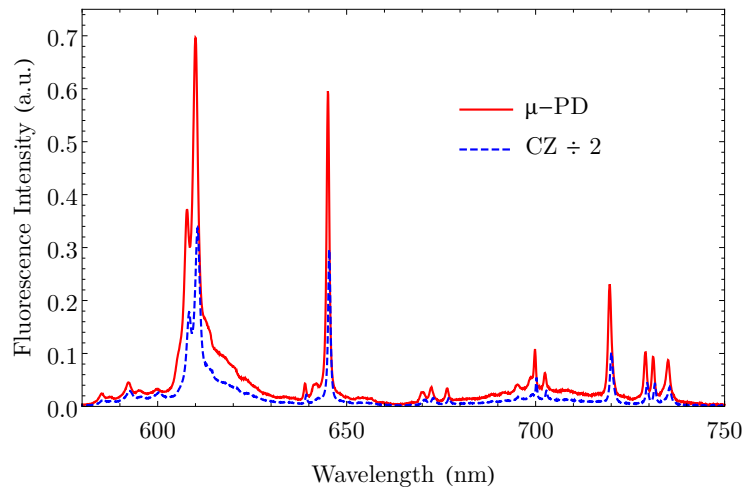
Figure 4. Fluorescence spectrum of our Pr:KYF SCF in the orange, red, and deep red regions, in comparison with a crystal grown by the CZ method. The spectrum of the CZ sample is scaled for clarity.

From the fluorescence decay time measurement, we obtained a single-exponential decay profile and an average lifetime of (39 ± 1) μs. These results are comparable with those reported for CZ-grown Pr:KYF samples [18], and also indicate the absence of non-radiative quenching.

3.3. Laser Experiments

Despite the large wedge angle between the circular facets, and despite the observed internal scattering, we achieved CW laser emission in the orange, red, and deep red regions. For each transition under investigation and for each choice of M2, we measured the output power as a function of the power absorbed by the sample, and with this data, we calculated the slope efficiency (η_{sl}) of the laser. In Table 1 we report, for each transition and for each choice of the transmittance of the mirror M2 (T_{M2}), the measured laser emission wavelength (λ_{out}), the slope efficiency (η_{sl}), the threshold power (P_{thr}), and the maximum output power (P_{out}). For all transitions, P_{out} corresponds to an absorbed pump power of 840 mW. As expected, all laser emissions were unpolarized. Figure 5 shows the data for three configurations in all the regions under investigation.

Table 1. Laser parameters for the transitions under investigation.

λ_{out}	T_{M2}	η_{sl}	P_{thr}	P_{out}
610 nm	1.2%	7%	204 mW	43 mW
645 nm	0.5%	3%	128 mW	17 mW
	1.8%	6%	134 mW	39 mW
	3.6%	8%	171 mW	47 mW
720 nm	1.0%	9%	186 mW	54 mW
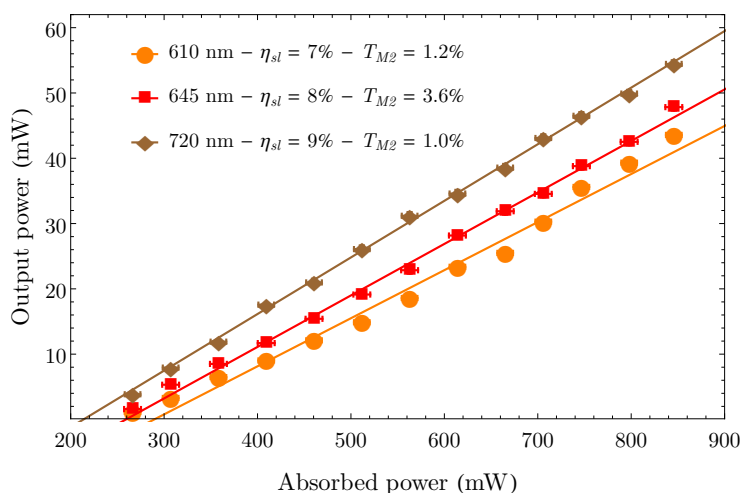
Figure 5. Output powers as functions of the absorbed pump power for three laser transitions of the Pr:KYF SCF, in the orange, red, and deep red regions.

Using the Findlay–Clay [19] and Caird [20] methods on the three slopes acquired for the red transition, we estimated the fraction of round-trip passive losses in the sample. The results of the two analyses were around 9% and 2%, respectively. The discrepancy between these two estimates comes from the fact that the first value is more affected by the poor shape and quality of the facets and by the large wedge angle, while the second is more influenced by the smaller propagation losses inside the sample. These passive losses are quite high in comparison with earlier reports on lasers based on CZ-grown Pr:KYF, which ranged from 0.3% to 5% [8,9,18,21], suggesting that the growth of KYF by the μ-PD method is not yet optimized.

As expected from the estimations of the passive losses, the laser performances of this SCF are worse than those previously reported for diode-pumped CZ-grown Pr:KYF lasers. In particular, the best slope efficiencies reported so far are about 18% in the orange region, about 23% in the red region, and about 24% in the deep red region [8,9,18]—much higher than the parameters obtained in this work. Given the poor propagation properties of our laser sample, those discrepancies were

expected. For the same reason, we did not investigate the propagation and the transverse profile of the output beams.

4. Conclusions

In this work, we succeeded in growing for the first time a KYF SCF by the μ-PD method. Despite the issues associated with the growth of this material by various techniques, we managed to grow a single crystal with a fairly transparent core. The grown crystal proved to be brittle and difficult to polish, and thus treated samples showed poor propagation properties. Hence, we did not manage to obtain flat and parallel circular facets in the sample prepared for laser experiments. It is not clear if these difficulties in preparing samples from this Pr:KYF SCF were due to the intrinsic fragility of this material when grown by the μ-PD method, or to the aforementioned problems occurring in the growth of this specific SCF. To answer this question, we intend to grow other KYF SCFs by the μ-PD method in the foreseeable future. Nevertheless, the spectroscopic features (absorption, steady-state, and dynamic fluorescence) of this SCF were measured and compared with the same characteristics of a CZ-grown Pr:KYF sample, showing no significant differences. Despite the polishing issues, we achieved laser emission on three lines, located in the orange, red, and deep red regions. To the best of our knowledge, we demonstrated for the first time the laser operation of a rare-earth-doped SCF of KYF grown by the μ-PD method. We obtained 44 mW at 610 nm, with a slope efficiency of 8%; 48 mW at 645 nm, with a slope efficiency of 9%; and 54 mW at 720 nm, with a slope efficiency of 10%. Our main goals for the future are to improve our growth procedures and to develop better polishing techniques that allow us to improve the flatness and the parallelism of the circular facets. These improvements will lead to an overall enhancement of the laser performances. Furthermore, we plan to investigate the effects of the local optical anisotropy of the doping site of KYF, studied in [15,22].

Author Contributions: J.S. performed the structural analyses and the spectroscopic characterizations; A.S. and M.T. conceived this work and designed the experimental setups; E.D. and A.S. built the resonator, performed the laser experiments, analyzed the data, and wrote the paper; Z.Z. performed the crystal growth of the SCF; M.T. contributed with materials and analysis equipment, designed the growth apparatus, and provided the facilities employed.

Conflicts of Interest: The authors declare no conflict of interest.

Abbreviations

The following abbreviations are used in this manuscript:

SCF	Single-crystal fiber
KYF	Potassium triyttrium decafluoride (KY_3F_{10})
CZ	Czochralski
μ-PD	Micro-pulling-down
CW	Continuous-wave

References

1. Smart, R.; Carter, J.; Tropper, A.; Hanna, D.; Davey, S.; Carter, S.; Szebesta, D. CW room temperature operation of praseodymium-doped fluorozirconate glass fibre lasers in the blue-green, green and red spectral regions. *Opt. Commun.* **1991**, *86*, 333–340.
2. Sandrock, T.; Danger, T.; Heumann, E.; Huber, G.; Chai, B. Efficient continuous wave-laser emission of Pr^{3+}-doped fluorides at room temperature. *Appl. Phys. B* **1994**, *58*, 149–151.
3. Kränkel, C.; Marzahl, D.T.; Moglia, F.; Huber, G.; Metz, P.W. Out of the blue: Semiconductor laser pumped visible rare-earth doped lasers. *Laser Photon. Rev.* **2016**, *10*, 548–568.
4. Sottile, A.; Damiano, E.; Tonelli, M. Diode-pumped laser operation of Pr^{3+}:Ba($Y_{0.8}Lu_{0.2}$)$_2F_8$ in the visible region. *Opt. Lett.* **2016**, *41*, 5555–5558.

5.   Hegarty, J.; Huber, D.L.; Yen, W.M. Fluorescence quenching by cross relaxation in LaF$_3$:Pr^{3+}. *Phys. Rev. B* **1982**, *25*, 5638–5645.

6.   Parisi, D.; Veronesi, S.; Tonelli, M. Method for Forming Bulk Crystals, in Particular Monocrystals of Fluorides Doped with Rare-Earth Ions. U.S. Patent 20120260846, 18 October 2012.

7.   Schellhorn, M.; Parisi, D.; Eichhorn, M.; Tonelli, M. Continuous-wave and Q-switched operation of a resonantly pumped Ho^{3+}:KY$_3$F$_{10}$ laser. *Opt. Lett.* **2014**, *39*, 1193–1196.

8.   Metz, P.W.; Müller, S.; Reichert, F.; Marzahl, D.T.; Moglia, F.; Kränkel, C.; Huber, G. Wide wavelength tunability and green laser operation of diode-pumped Pr^{3+}:KY$_3$F$_{10}$. *Opt. Express* **2013**, *21*, 31274–31281.

9.   Sottile, A.; Metz, P.W. Deep red diode-pumped Pr^{3+}:KY$_3$F$_{10}$ continuous-wave laser. *Opt. Lett.* **2015**, *40*, 1992–1995.

10.   Yoshikawa, A.; Chani, V. Growth of Optical Crystals by the Micro-Pulling-Down Method. *MRS Bull.* **2009**, *34*, 266–270.

11.   Fukuda, T.; Chani, V. *Shaped Crystals: Growth by Micro-Pulling-Down Technique*; Advances in Materials Research; Springer: Berlin/Heidelberg, Germany, 2007.

12.   Sottile, A.; Zhang, Z.; Veronesi, S.; Parisi, D.; Lieto, A.D.; Tonelli, M. Visible laser operation in a Pr^{3+}:LiLuF$_4$ monocrystalline fiber grown by the micro-pulling-down method. *Opt. Mater. Express* **2016**, *6*, 1964–1972.

13.   Damiano, E.; Shu, J.; Sottile, A.; Tonelli, M. Spectroscopy and visible laser operations of a μ-PD grown Pr^{3+}:LiYF$_4$ single-crystal fiber. *J. Phys. D Appl. Phys.* **2017**, *50*, 135107.

14.   McMillen, C.D.; Comer, S.; Fulle, K.; Sanjeewa, L.D.; Kolis, J.W. Crystal chemistry of hydrothermally grown ternary alkali rare earth fluorides. *Acta Cryst.* **2015**, *71*, 768–776.

15.   Wells, J.P.R.; Yamaga, M.; Han, T.P.J.; Gallagher, H.G. Infrared absorption, laser excitation and crystal-field analyses of the C$_{4v}$ symmetry centre in KY$_3$F$_{10}$ doped with Pr^{3+}. *J. Phys. Condens. Matter* **2000**, *12*, 5297.

16.   Nehari, A.; Duffar, T.; Ghezal, E.; Lebbou, K. Chemical Segregation of Titanium in Sapphire Single Crystals Grown by Micro-Pulling-Down Technique: Analytical Model and Experiments. *Cryst. Growth Des.* **2014**, *14*, 6492–6496.

17.   Veronesi, S.; Zhang, Y.; Tonelli, M.; Schellhorn, M. Efficient laser emission in Ho^{3+}:LiLuF$_4$ grown by micro-Pulling Down method. *Opt. Express* **2012**, *20*, 18723–18731.

18.   Camy, P.; Doualan, J.L.; Moncorgé, R.; Bengoechea, J.; Weichmann, U. Diode-pumped Pr^{3+}:KY$_3$F$_{10}$ red laser. *Opt. Lett.* **2007**, *32*, 1462–1464.

19.   Findlay, D.; Clay, R.A. The measurement of internal losses in 4-level lasers. *Phys. Lett.* **1966**, *20*, 277–278.

20.   Caird, J.A.; Payne, S.A.; Staber, P.R.; Ramponi, A.J.; Chase, L.L.; Krupke, W.F. Quantum electronic properties of the Na$_3$Ga$_2$Li$_3$F$_{12}$:Cr^{3+} laser. *IEEE J. Quant. Electron.* **1988**, *24*, 1077–1099.

21.   Xu, B.; Camy, P.; Doualan, J.L.; Cai, Z.; Moncorgé, R. Visible laser operation of Pr^{3+}-doped fluoride crystals pumped by a 469 nm blue laser. *Opt. Express* **2011**, *19*, 1191–1197.

22.   Metz, P.W.; Calmano, T.; Marzahl, D.T.; Kraenkel, C.; Huber, G. Polarization Effects in Pr^{3+}-Doped Cubic KY$_3$F$_{10}$ and Stable Dual Wavelength Lasing. In *Advanced Solid State Lasers*; Optical Society of America: Washington, DC, USA, 2015; p. ATu1A.3.